SCIENCE CHINA
Earth Sciences

•REVIEW•

February 2021 Vol.64 No.2: 191–204
https://doi.org/10.1007/s11430-020-9672-7

Tsunamis and tsunami warning: Recent progress and future prospects

Chao AN*

Key Laboratory of Hydrodynamics (Ministry of Education), School of Naval Architecture, Ocean and Civil Engineering, Shanghai Jiao Tong University, Shanghai 200240, China

Received April 12, 2020; revised June 22, 2020; accepted July 8, 2020; published online November 6, 2020

Abstract Tsunamis are one of the most destructive disasters in the ocean. Large tsunamis are mostly generated by earthquakes, and they can propagate across the ocean without significantly losing energy. During the shoaling process in coastal areas, the wave amplitude increases dramatically, causing severe life loss and property damage. There have been frequent tsunamis since the 21st century, drawing the attention of many countries on the study of tsunami mechanism and warning. Tsunami records also play an essential role in deriving earthquake rupture models in subduction zones. This paper reviews the recent progress and limitations of tsunami research, from the aspects of tsunami generation, propagation, inversion and warning. Potential tsunami warning strategies are discussed and future prospects on tsunami research are provided.

Keywords Tsunamis, Tsunami warning, Tsunami inversion, Subduction earthquakes, Tsunami simulation

Citation: An C. 2021. Tsunamis and tsunami warning: Recent progress and future prospects. Science China Earth Sciences, 64(2): 191–204, https://doi.org/10.1007/s11430-020-9672-7

1. Introduction

Tsunamis are gravitational water waves in the ocean, which can be generated by thrust earthquakes in subduction zones, submarine landslides and volcano eruptions. Tsunamis have very long wavelengths and relatively small amplitudes in the open ocean, and hence they can travel large distances without significant energy losses. During the runup process in shallow water near coastlines, the shoaling effects lead to wavelength decreasing and dramatic amplitude increasing, causing severe damage to coastal residents and facilities. Tsunamis occurred many times in history and left geological signatures such as tsunami deposits. They were also recorded by historical documents (e.g., Satake et al., 2020). Since modern instruments of measuring water height were invented, there are more and more quantitative observations and scientific research on tsunamis.

Tsunamis that occur prior to the historical record or for which there are no written observations are called paleotsunamis. Tsunamis that are documented to occur through eyewitness or instrumental observation within the historical record are called historical tsunamis. Research on paleotsunamis generally depends on tsunami deposits in coastal regions to infer the occurring time and inundation area. For historical tsunamis, in addition to tsunami deposits, historical documents about tsunami damage can also be analyzed to estimate the wave characteristics. For instance, according to the Japanese historic records about wave damage to houses and facilities in AD 1700, Satake et al. (1996) estimated the tsunami wave height and arrival time, and then inferred that the tsunami source was a *M*9 earthquake in the Cascadia subduction zone along the west coast of North America. Later Yamaguchi et al. (1997) conducted analysis of tree-ring dating in the Cascadia coast and demonstrated that the trees were killed as a result of a *M*9 earthquake in AD 1700. Nanayama et al. (2003) studied the coastal deposits in

* Corresponding author (email: anchao@sjtu.edu.cn)

Eastern Hokkaido, Japan, and found evidence for a large earthquake every 500 years in the past 2000–7000 years. Monecke et al. (2008) analyzed the deposits in Northern Sumatra, and showed that two historic events left deposits with similar characteristics as the 2004 Sumatra tsunami deposits, implying that there could have been two large tsunamis in approximately AD 1290–1400 and AD 780–990. Sun et al. (2013) showed evidence for a possible large tsunami in AD 1024 in the South China Sea according to the deposits in Xisha islands. Namegaya and Satake (2014) studied the AD 869 Jogan, Japan earthquake and inferred that the magnitude of the earthquake was at least M_W8.6, based on analysis of the area and depth of tsunami deposits, in combination with numerical simulations. The 869 Jogan earthquake is the predecessor of the 2011 Tohoku earthquake, and its magnitude is a key factor to understand the recurrence interval of giant earthquakes in this region.

Observations of paleotsunamis and historical tsunamis are inadequate, and data accuracy is relatively poor, which greatly limits the research on these tsunamis. In 1851 the first self-recording tide gauge was deployed in San Francisco, U. S., and since then there have been more and more quantitative measurements of tsunamis. The first two large tsunamis that were recorded by an instrument were the 1854 Tokai and Nankai, Japan tsunamis, which occurred on December 23 and 24 in 1854, respectively, approximately 30 hours apart. The magnitude of both of the two earthquakes was estimated to be around 8.4, and both earthquakes occurred in the Nankai subduction zone in Southern Japan. Earthquake-triggered tsunamis propagated across the Pacific Ocean and reached San Francisco after about 12.5 hours, where they were recorded by a local tide gauge. The recordings show that the amplitude of the two tsunamis was about 10 cm, which was much smaller than the tide amplitude of about 2 m. The measurements have been digitalized and can be accessed from the website of the National Oceanic and Atmospheric Administration (NOAA) (https://www.ngdc.noaa.gov/hazard/tide.shtml). Later, two more giant earthquakes occurred at similar locations in this subduction zone, i.e., the 1944 *M*8.1 Tonankai earthquake and the 1946 *M*8.3 Naikai earthquake. Both earthquakes excited tsunamis, which were recorded by multiple tide stations in Japan, with maximum wave amplitudes of about 1 m. The tsunami data were later used to study the rupture area and slip distribution of the earthquakes (Satake, 1993; Tanioka and Satake, 2001a, 2001b; Baba et al., 2002; Baba and Cummins, 2005). These measurements are important evidences to constrain the earthquake cycle in the Nakai subduction zone. Whether the 1944 and 1946 earthquakes released all the energy accumulated since the two 1854 earthquakes, when the next giant earthquake will occur in the Naikai subduction zone and how large a tsunami will be triggered are hot research topics on Japan's earthquakes and tsunamis (e.g., Mulia et al., 2017b; Watanabe et al., 2018). Another instrument-recorded large tsunami was the 1993 Krakatoa tsunami in Indonesia, which was generated by volcano eruption and killed more than 36000 people (Simkin and Fiske, 1983). After the eruption of the Krakatoa volcano in 1883, magma gradually accumulated and formed another volcano called Anak Krakatoa, which literally means "the son of Krakatoa". The new volcano erupted again on December 22nd, 2018, led to obvious landslides (Williams et al., 2019) and triggered a large tsunami, killing more than 400 people (Grilli et al., 2019). Besides, the 1960 Chilean tsunami was generated by a *M*9.5 earthquake, which was the largest earthquake ever recorded. The tsunami was recorded at multiple tide gauges in Chile, United States and Japan, and the tsunami data were used to constrain the earthquake source models (Ho et al., 2019). The 2004 Sumatra tsunami was triggered by a *M*9.2 earthquake with a rupture length of more than 1000 km. The largest runup height of the tsunami waves was about 30 m, leading to more than 230000 deaths. The tsunami was recorded by a dense network of tide gauges, as well as satellite, and the measurements were used to study the earthquake rupture process and tsunami source (Lay et al., 2005; Titov et al., 2005; Liu et al., 2005; Wang and Liu, 2006; Fujii and Satake, 2007).

The 2004 Sumatra tsunami drew the attention of many countries on the research of tsunamis and tsunami warning. Observation techniques have also improved since the event. For tsunami warning purposes, NOAA deployed multiple tsunami buoys in the open ocean, known as the DART project (deep-ocean assessment and reporting of tsunamis). The recording instrument of a tsunami buoy is a pressure sensor sitting on the seafloor, which measures ocean-bottom pressure. As a tsunami wave passes by, it causes water height change above the pressure sensor, and in consequence the change of ocean-bottom pressure. The pressure change is then converted to tsunami wave height using the formula of static water pressure. Measurements are transmitted to the buoy on the sea surface through water sounds, and then sent to satellite, and then the data center on land, where the data are analyzed for tsunami warning purposes. The whole process can be accomplished in real time. Tsunami measurements at buoys can be found from NOAA's website (https://nctr.pmel.noaa.gov/dart). Tsunami buoys are generally deployed near trenches in subduction zones in order to detect tsunami waves as soon as possible after an earthquake. Tsunami data recorded at tsunami buoys are not significantly affected by ocean bathymetry, which can be used to constrain earthquake source models, providing essential information for the study of subduction earthquakes. In addition, traditional tide gauges, which are generally deployed near coastlines, also record tsunami waves. Although the data especially the trailing waves can be affected by local bathymetry, they are also used for earthquake source studies.

Tide gauge data can be accessed from the website of the Intergovernmental Oceanographic Commission (IOC, http://www.ioc-sealevelmonitoring.org). Tsunami data recorded at tsunami buoys and tide gauges, along with other types of data, such as seismic waves, geodetic data, etc., have been widely used to jointly constrain the rupture process of subduction earthquakes since 2004, such as the 2010 Maule earthquake (Fujii and Satake, 2013; Yue et al., 2014), the 2011 Tohoku earthquake (Fujii et al., 2011; Satake et al., 2013), the 2014 Iquique earthquake (An et al., 2014; Lay et al., 2014), and the 2015 Illapel earthquake (Heidarzadeh et al., 2016; An et al., 2017b).

China owns more than 18000 kilometers of mainland coastline and governs more than 3 million square kilometers of sea area, but there have been relatively few historical tsunamis. According to NOAA's tsunami database (https://www.ngdc.noaa.gov/hazard/tsu_db.shtml), Figure 1 summarizes all the confirmed tsunamis in Asia-Pacific marginal seas generated by earthquakes or volcanoes. Figure 1 shows that the tsunami threats to China are mainly from the Manila and Ryukyu-Nankai subduction zones. The Manila subduction zone, where the Sunda Plate subducts beneath the Philippine Sea Plate at a speed of about 50–100 mm yr^{-1} (Hsu et al., 2012, 2016), is a focused area for tsunami research surrounding the South China Sea (e.g., Liu et al., 2007; Liu et al., 2009; Megawati et al., 2009; Ren et al., 2014; Li et al., 2016). There have been frequent earthquakes in the Manila subduction zone in history, but there are no direct evidences of a tsunami. Sun et al. (2013) inferred that a large tsunami occurred in the South China Sea around AD 1024 by analyzing the deposits in Xisha islands. Yang et al. (2017, 2019) investigated more deposits and archaeological findings, and suggested that the tsunami occurred in AD 1076 and originated from the Manila subduction zone. Since 2007 the South Tsunami Sea Tsunami Workshop has been held annually, focusing on the study of potential tsunamis in the Manila subduction zone, discussing possible fault parameters, tsunami warning strategies around the South China Sea and tsunami's impact on coastal engineering. The State Oceanic Administration of China started the building of the South China Sea tsunami warning center in 2013, and began to provide 24-hour tsunami warning service in 2018 to countries surrounding the South China Sea. The Manila subduction zone is a key monitoring zone for the warning center. Large tsunamis occurred many times in the Ryukyu trench to the north of Taiwan, such as the 1771 tsunami, which killed more than 10000 people (Nakamura, 2009). Further north in the Nankai trench, Japan, tsunamis were even more severe in history. So far there have been very few studies on the impact of tsunamis in the Ryukyu and Nankai trenches to China. The Izu-Bonin and the Mariana trenches to the east, and the Philippine trench to the south hosted small to moderate tsunamis in history, which had limited impact on China. Tsunamis in the Sumatra zone to the southwest are frequent and usually large, but the impact on China is negligible due to the blockage of waves by islands in Southeast Asia.

Tsunamis are mostly generated by earthquakes, landslides, volcano eruptions, etc.. Generally speaking, earthquake-generated tsunamis are more frequent, and in light of the global tsunami observation system, the current research on the mechanism and warning of such tsunamis is relatively well developed. This paper reviews the recent research progress of earthquake-generated tsunamis, from the aspects of generation, propagation, inversion and warning, and discusses future prospects of research hotspots.

2. Tsunami generation

Tsunami generation by a thrust earthquake is a complex process that involves fault rupture, seafloor deformation and seawater response, producing seismic waves, permanent deformation, sea-surface height change and ocean-bottom pressure change. Figure 2 is a schematic diagram showing the process of tsunami generation. As the oceanic plate subducts beneath the continental plate, the fault at the plate boundary ruptures and triggers an earthquake, which radiates seismic waves and causes deformation of land and seafloor. The deformation on land can be measured by GNSS and radar, while the deformation in the sea leads to vertical movement of the seawater, which then propagates outwards as tsunami waves. Later tsunami waves are recorded by ocean-bottom pressure sensors deployed on the seafloor, as well as tide gauges near coastlines. Besides, because the seawater is compressible, there exist elastic waves in the seawater, i.e., water sound waves. Water sound waves are generated by the force exerted on the seawater by seafloor deformation, and also the transmission of seismic waves at the solid-fluid interface.

The generation of a tsunami involves the coupling of solid Earth and fluid, but a common practice is to decouple the process, analyze the fault rupture first, and then utilize the results as boundary conditions to study the response of the water. One widely-used simplified model ignores the temporal process of the fault rupture, and calculates the permanent seafloor deformation resulting from the final slip based on a half-space elastic model (Okada, 1985). This model also assumes that the seawater simultaneously responds to the seafloor deformation, and that the sea-surface height mimics the seafloor deformation. Thus, the initial height of the sea surface is obtained, and the propagation and inundation of tsunami waves are studied by water wave theories. In this paper this model is referred to as the static elevation model. The assumptions made by this model and the resulting errors are discussed in this section.

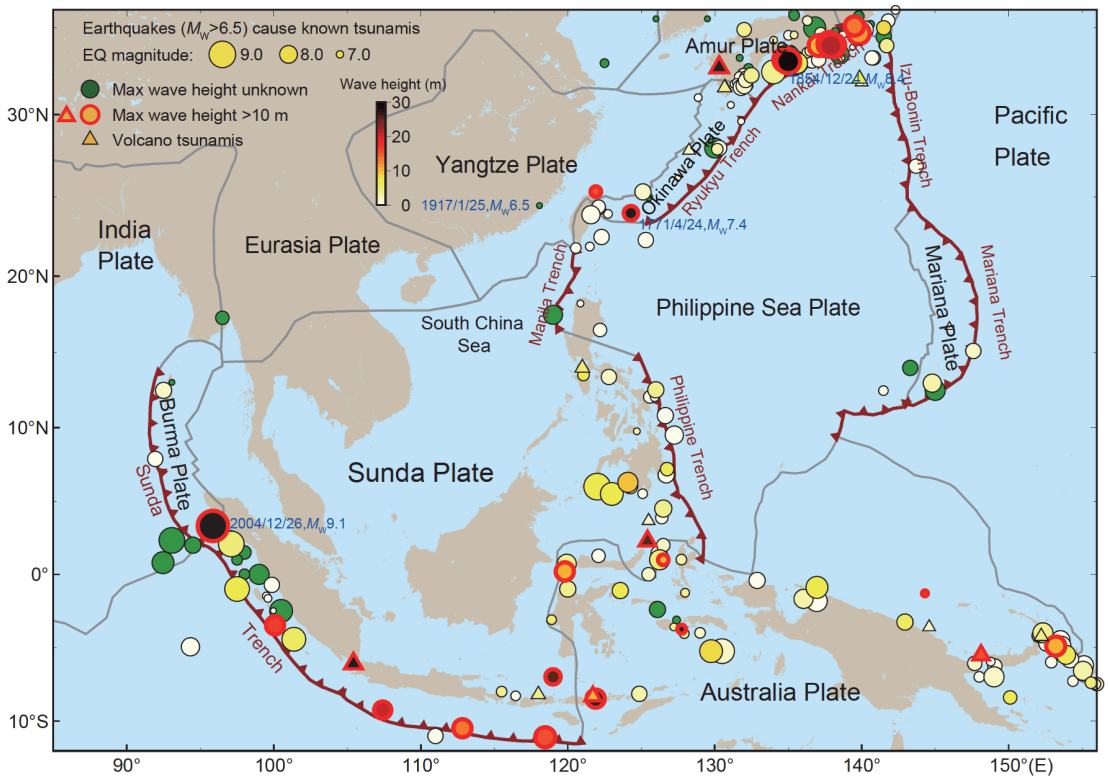

Figure 1 Historical tsunamis in Asia-Pacific marginal seas. Circles denote earthquake-triggered tsunamis, and the size indicates the earthquake magnitude. Triangles represent volcano-generated tsunamis. Filled colors show the known water height. Symbols with a red outer line indicates a water height greater than 10 m. Data source: NOAA's tsunami data base (https://www.ngdc.noaa.gov/hazard/tsu_db.shtml).

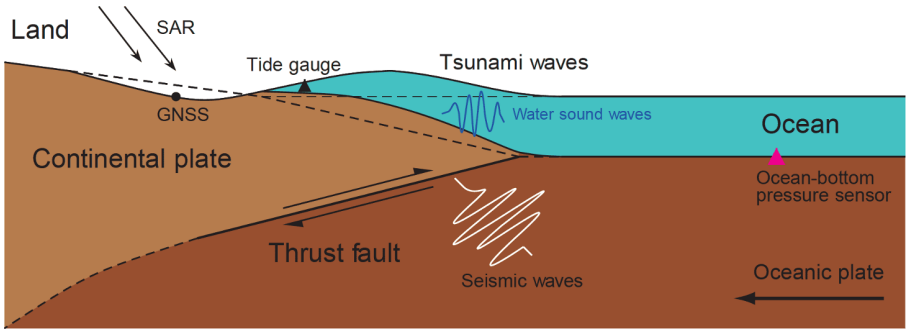

Figure 2 A schematic diagram showing the generation of a tsunami by a thrust earthquake. The oceanic plate subducts beneath the continental plate from right to left, and a thrust earthquake occurs at the plate boundary. The earthquake radiates seismic waves (in white), and causes land and seafloor deformation (dashed and solid lines). Seafloor deformation leads sea-surface height change, which propagates outwards as tsunami waves. Seafloor deformation and seismic waves also generate water sound waves in the seawater (in blue).

2.1 Impact of earthquake rupture process on tsunami generation

The static elevation model ignores the temporal earthquake rupture process and uses the permanent seafloor deformation as the initial condition for the seawater. The basis is that earthquake rupture time is generally much smaller than the period of tsunami waves. For instance, the rupture time of an earthquake of magnitude 8.5 is about 1 min. The resulting tsunami waves are gravitational water waves, the wavelength is similar to the earthquake rupture extent, and the propagating speed is $\sqrt{gh}$ (g gravitational acceleration, h water depth). So the period of tsunami waves is about 20 min assuming a wavelength of 150 km and water depth of 2.0 km. During the 1-min earthquake rupture time, the propagation time for the tsunami waves is only 1/20 periods, leading to negligible propagation effects. Fujii et al. (2011) ignored the rupture process of the 2011 Tohoku earthquake and inverted the tsunami data to derive the final slip distribution. To account for the effects of rupture process, it is necessary to discretize the process in time, calculate the tsunami generation for each time segment, and superimpose the newly

generated tsunami waves on the propagation of previously-generated tsunami waves. For example, Satake et al. (2013) proposed a source model with a rupture time of about 3 min for the 2011 Tohoku earthquake, and claimed that the model predicts later and lower tsunami waves in the near field, which match observations better than instant rupture models. Generally speaking, the larger the earthquake magnitude, the longer the fault rupture length, the longer the rupture time, and the more significant the impact of the rupture process on tsunami generation. Taking the 2004 Sumatra earthquake as an example, it ruptured approximately 1300 km and the rupture duration was about 8 min (Ishii et al., 2005). Thus it is necessary to consider the rupture process to study this event (e.g., Grilli et al., 2007; Fujii and Satake, 2007). It should be noted that, although tsunami waves are affected by the earthquake rupture process, tsunami data have low accuracy in resolving the temporal rupture process (Fujii and Satake, 2007). Ren et al. (2019) conducted numerical simulations and demonstrated that earthquake rupture process affected the tsunami generation significantly for rupture length of 1000 km or larger.

2.2 Relationship between sea-surface height and seafloor deformation

The static elevation model assumes that the initial sea-surface height mimics the vertical seafloor deformation. This assumption is discussed in three aspects in the following text. First, does the vertical seafloor deformation lead to the same sea-surface height change? Assuming incompressible seawater, the fluid can be treated as potential fluid. The depth that a surface water wave can influence is the same order of the wavelength. Similarly, the depth that the seafloor deformation can influence is also the same order of the deformation length. If the seafloor deformation has a very small horizontal scale, it cannot penetrate the water layer and cause any sea-surface height change. If the horizontal scale of the seafloor deformation is much larger than the water depth, the sea-surface height change will be exactly the same as the vertical seafloor deformation. In other words, short-wavelength components in the seafloor deformation are attenuated when converted to sea-surface height change. The shorter the wavelength, the heavier the attenuation, which is similar to a low-pass filter. Japanese scientist Kinjiro Kajiura carried out pioneer work on the theories of tsunami generation (Kajiura, 1963, 1970, 1981), so the formula to account for such an effect is also called the "Kajiura's equation" (Kajiura, 1963), which has been applied to realistic tsunami simulations (e.g., Tanioka and Seno, 2001; Gusman et al., 2012). In general, the horizontal scale of seafloor deformation caused by large earthquakes is similar to the earthquake rupture extent, which is much larger than water depth. So this effect is significant for small earthquakes and large water depths.

Second, in addition to the vertical deformation, the horizontal displacement also contributes to tsunami generation if the seafloor is tilted. Tanioka and Satake (1996) proposed a formula to quantitatively calculate the sea-surface height change due to the horizontal displacement. The idea is straightforward, i.e., the sea-surface height change is equal to the product of the horizontal seafloor displacement and the tangent of seafloor sloping angle. The formula is widely used in numerical simulations of real tsunamis (e.g., Fujii and Satake, 2007; Satake et al., 2013). The dipping angle of the faults in subduction zones is in general small near the trench (about 10°). Therefore, the horizontal displacement of the seafloor is usually greater than the vertical displacement during a thrust earthquake. As a result, if the slope of the seafloor is steep, the contribution of the horizontal seafloor displacement to tsunami generation can be close to that of the vertical displacement. For example, Satake et al. (2013) suggested that the horizontal displacement contributed 20–40% of the tsunami height at some near-field stations in the 2011 Tohoku tsunami. Hu et al. (2020) conducted numerical simulations and verified that the formula proposed by Tanioka and Satake (1996) is valid for both compressible and incompressible seawater.

Third, does the horizontal velocity of the seawater, which is caused by the horizontal motion of a tilted seafloor, contribute to tsunami generation? Most studies assume that the initial velocity field in the seawater is zero, and tsunamis are generated only by the initial sea-surface elevation. Song et al. (2008, 2017) argued that, the horizontal movement of a tilted seafloor will produce a horizontal velocity field in the seawater, and that such a horizontal velocity may significantly affect the tsunami generation. They carried out experimental and numerical analysis, and suggested that the horizontal velocity field accounted for 2/3 of the height of the 2004 Sumatra tsunami, and 1/2 of the 2011 Tohoku tsunami. The results are somewhat controversial. One reason is that the theory adopted by Song et al. (2017) was derived for vertical walls, while the slope of a realistic seafloor is mild. Lotto et al. (2017) considered seawater compressibility and solid-fluid coupling, and numerically simulated the complete process of earthquake rupture and tsunami generation. Their results showed that the horizontal velocity field resulting from the horizontal seafloor motion is elastic waves, which carry away the energy when propagating outwards from the source region, and do not contribute to the tsunami height. Hu et al. (2020) conducted similar numerical analysis and verified that the horizontal velocity field in the seawater is negligible to tsunami generation. Therefore, the horizontal velocity field in the seawater is elastic waves that are decoupled with gravitational tsunami waves, and can be ignored for tsunami generation. The contribution of the horizontal motion of a tilted seafloor can be accurately

evaluated by the formula of Tanioka and Satake (1996).

2.3 Impact of seawater compressibility on tsunami generation

Most tsunami generation models assume that the seawater is incompressible. The assumption is based on the fact that the speed of water sound waves is much larger than that of tsunami waves. For instance, sound speed in water is about 1.5 km s^{-1}, while tsunami speed is about 0.14 km s^{-1} for a water depth of 2000 m. Thus, sound and tsunami waves overlap in the source region, but they will separate shortly and do not affect each other after separation (Hu et al., 2020). In reality, tsunami buoys are being deployed more and more closely to earthquake sources, and for future tsunami buoys there could be not enough time for the two different waves to separate. Thus, future records will be the superposition of seismic waves, water sound waves and tsunami waves. Hence, it is essential to extract the tsunami information in the records for tsunami warning purposes (Saito, 2013, 2017; Saito and Tsushima, 2016). Water compressibility must be considered to analyze the seismic and water sound waves in the records, especially for high-frequency components (An et al., 2017a). The current sampling rate of tsunami buoys is low (15 s to 1 min per sample), which greatly limits the research in this field due to limited observations. When considering seawater compressibility, seismic waves transmit at the solid-fluid boundary to water sound waves, and permanent seafloor deformation also generates water sound waves. An essential criterion for judging whether an earthquake generates a tsunami is whether it causes large seafloor deformation. In this sense, detecting and analyzing the water sound waves generated by seafloor deformation will be direct basis for fast tsunami alert (Nosov, 1999; Nosov and Kolesov, 2007; Mei and Kadri, 2018). For example, Mei and Kadri (2018) investigated the sound waves generated by a slender fault through a perturbation approach, and obtained an asymptotic theoretical solution of sound waves propagating in space. Nevertheless, their work only considered the fluid. Sound waves were generated by the boundary condition imposed at the bottom boundary, and seismic waves radiated by the earthquake in the underlying elastic Earth were ignored. These seismic waves can also generate sound waves by transmission at the solid-fluid boundary. Therefore, it is important to distinguish between sound waves generated by seafloor deformation and seismic waves. By considering earthquake rupture and seismic waves, it is difficult to derive theoretical solutions. Thus, numerical approaches are preferred to study the characteristics of water sound waves. Realistic observations are also very important. With the development of Japanese ocean-bottom observation network (S-net), and the deployment of more DART buoys in source areas with high sampling rate, the study of ocean-bottom pressure recordings and the response of compressible seawater during an earthquake can be a promising research field in the future.

3. Tsunami propagation

The propagation of tsunamis can be described by classic water wave theories in general. Neglecting water viscosity and assuming potential fluid, the velocity potential satisfies the Laplace equation (Wu, 1982). The boundary conditions are the kinetic and dynamic free surface boundary conditions, and the continuity of vertical velocity at the seabed boundary. Thus, all the governing equations of water waves are obtained (e.g., Mei, 1989). Two dimensionless parameters can be introduced to describe the characteristics of water waves, i.e., $\varepsilon=A/h$, $\mu^2=(kh)^2$, which represent wave nonlinearity and dispersion, respectively. A, h and k are characteristic wave amplitude, water depth and wave number, respectively. If both ε and μ^2 are small and they are of the same order of magnitude, the governing equations can be expanded as a power series in the vertical direction. Then, by neglecting high-order terms, the three-dimensional governing equations are reduced to two-dimensional Boussinesq equations in the two horizontal coordinates. If nonlinearity is retained and dispersion is neglected, the governing equations are simplified to nonlinear shallow water wave equations. If both nonlinearity and dispersion are neglected, Boussinesq equations are simplified to linear shallow water wave equations.

The amplitude of tsunami waves generated by large subduction thrust earthquakes is about 1 m in the open ocean, the water depth is about 4 km and the wavelength is about 100 km, leading to very small ε and μ^2. Thus, nonlinearity and dispersion are weak for tsunami waves (An and Liu, 2014). Although some studies claim that wave dispersion could be important even in the near field (e.g., Saito et al., 2011, 2014), shallow water wave equations that neglect wave dispersion are widely adopted to study tsunamis generated by large thrust earthquakes, while Boussinesq equations of weak dispersion are used for relatively small tsunamis with wavelength comparable to water depth, such as landslide and volcano tsunamis. When tsunami waves propagate to nearshore areas, water depth decreases and wave amplitude increases, so wave nonlinearity becomes important. Therefore, nonlinear shallow water wave equations are commonly used to calculate the runup and inundation of tsunamis. Tsunami simulation packages that are developed based on linear and nonlinear shallow water wave equations include COMOCT (Liu et al., 1998; Wang and Liu, 2006), GEOCLAW (LeVeque et al., 2011), MOST (Titov and Gonzalez, 1997; Titov and Synolakis, 1998) and TUNAMI (Imamura, 1996). Numerical packages that solve Boussinesq equations are mainly

FUNWAVE (Shi et al., 2012), COULWAVE (Lynett and Liu, 2002) and Jagurs (Baba et al., 2017).

In numerical simulations of real tsunamis, it is found that the arrival time of tsunami waves is always earlier than observations. This phenomenon is particularly obvious at trans-ocean far-field stations, and the time difference can reach 15–30 min (e.g., Watada et al., 2014). The reason is that shallow water wave equations describe the propagation of tsunami waves under ideal conditions. In the real ocean, tsunami waves are affected by many factors, such as wave dispersion, Earth elasticity, water compressibility, seawater stratification due to temperature, salinity and pressure, and gravity change due to water wave propagation. These effects are small and negligible in the near field, but they accumulate in distance and become significant in the far field. Tsai et al. (2013), Watada (2013), An and Liu (2016) investigated the theoretical propagation speed of tsunami waves considering various factors. Yue et al. (2014) developed an approach in order to obtain accurate tsunami simulations. In the approach, tsunami waves were simulated using shallow water wave equations, and then the arrival time error induced by ignoring wave dispersion was calibrated according to the water depth along the travel paths of waves. Watada et al. (2014) adopted a similar strategy, i.e., in order to obtain accurate arrival time and waveforms, they used shallow water wave equations to simulate the tsunami waves, and then calibrated the various factors that affect tsunami propagation speed according to the travel paths of waves. By this means, tsunami waves in the far field can be accurately simulated, and hence far-field tsunami measurements can be adopted to study earthquake source parameters. This is a newly developed direction in tsunami research (e.g., Yue et al., 2014; Ho et al., 2017, 2019).

4. Tsunami inversion

Tsunami inversion refers to the inversion of tsunami observations to constrain the tsunami source, such as earthquake rupture process or initial sea-surface elevation. By adopting the static elevation model for tsunami generation, fault slip is linearly related to vertical seafloor deformation or initial sea-surface elevation; by adopting linear shallow water wave equations, initial sea-surface elevation is linearly related to tsunami waveforms recorded at tsunami stations. Thus, if ignoring the earthquake rupture process, or the earthquake rupture speed is known, the inversion of tsunami data for fault slip distribution is simply a linear inversion (Satake, 1987; Liu et al., 2009). Many studies of the source mechanisms of subduction earthquakes have demonstrated that, tsunami data are crucial to constrain the slip distribution, especially the amount of slip in the shallow portion near the trench. The reason is that the slip of large subduction earthquakes is usually shallow, and the resulting permanent seafloor deformation is mostly in the ocean, which later evolves to tsunami waves (Figure 3). Currently there is little direct measurement of the seafloor deformation, so the tsunami observations that originate from the seafloor deformation become very important. If only seismic waves and on-land geodetic data are used, it is not sufficient to accurately constrain the shallow slip on the fault. For example, An et al. (2014) found that, for the 2014 Iquique earthquake, slip models that were derived by only adopting far-field seismic data had large slip in both the shallow and deep portions of the fault. This led to two tsunami peaks, which were inconsistent with in-situ observations. For this earthquake, inversion of tsunami data revealed that the slip was concentrated in the deep portion near the hypocenter. Lay et al. (2014) also compared inversions of seismic and tsunami data, and drew similar conclusions for this event. Yue et al. (2014) performed joint inversions of multiple types of data for the 2010 Maule earthquake, and concluded that tsunami data can effectively constrain the shallow slip near the trench for large subduction earthquakes.

As there are more and more tsunami measurements, tsunami data are now widely used in the study of earthquake sources, and the joint inversion of multiple types of data becomes a popular method. Nevertheless, there are very few studies on the capability of tsunami data in resolving source details (e.g., Yue et al., 2020). For example, Fujii et al. (2011) divided the rupture area into patches of size of 50 km×50 km when inverting tsunami data for the 2011 Tohoku earthquake. In their later work, Satake et al. (2013) used smaller patches near the trench, which was 50 km×25 km. For the same earthquake, Simons et al. (2011) adopted a subfault size of about 20 km. An et al. (2018a) analyzed the 2011 Tohoku, 2014 Iquique and 2015 Illapel earthquakes and found that tsunami data have a low resolving capability of the slip distribution. For example, for the 2011 Tohoku earthquake, they constructed and compared two source models. One was a finite-fault model derived by inverting tsunami data and the subfault size was 25 km×25 km. The other was a uniform rectangular model obtained through a global search. The two source models predicted almost the same tsunami waveforms at 28 tsunami stations. They hence concluded that tsunami data were insensitive to earthquake source details. For more historic and future earthquakes, it is necessary to study the capability of tsunami data in resolving earthquake source details, which is important because it determines whether the source details derived from an inversion can be interpreted correctly. Besides, different studies use different amount of tsunami data. For the 2011 Tohoku earthquake, Fujii et al. (2011) adopted data from 33 tsunami stations, Simons et al. (2011) used 12 DART buoys and Satake et al. (2013) used 53 tsunami stations. Using more data in an inversion generally leads to better inversion

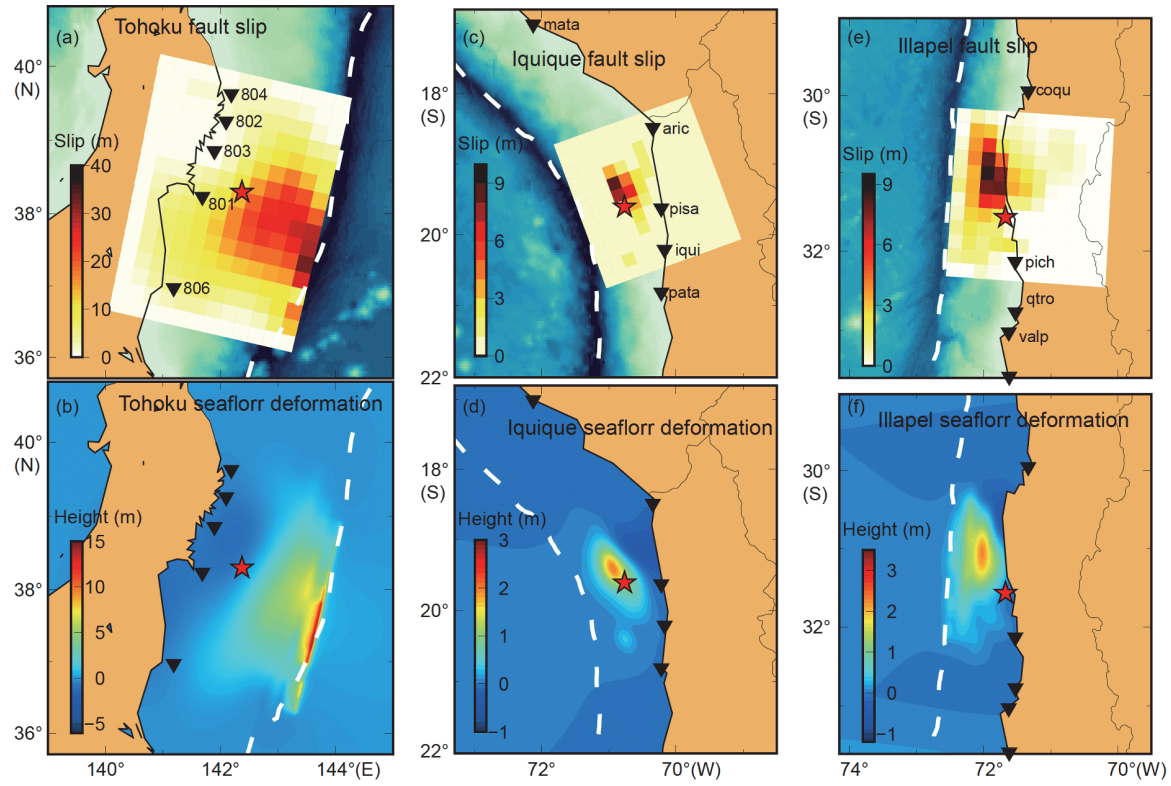

Figure 3 The slip distribution and seafloor deformation for the 2011 Tohoku, 2014 Iquique and 2015 Illapel earthquakes. Black inverted triangles denote the near-field gauges. Red star marks the epicenter. From the three earthquakes it is observed that, the permanent deformation of the Earth surface is mostly located in the ocean. The percentage of deformation in the ocean depends on the location of the slip, and the distance between the trench and the coast. The deformation in the ocean is later measured through tsunami waves, which play an important role in studying earthquake source mechanisms.

results. However, An et al. (2018b) analyzed the data at 28 tsunami stations in the Tohoku event and found that, if the azimuthal coverage of tsunami stations is good, and if the number of stations is equal to or more than 4, adding more tsunami data into the inversion does not improve the inversion results significantly. This conclusion is consistent with the above-mentioned statement that tsunami data have low resolution of the slip distribution., i.e., tsunami data carry relatively simple earthquake source information.

Traditional tsunami inversion derives earthquake rupture parameters from tsunami data. There are other methods that separate tsunamis from earthquakes. These methods ignore the earthquakes, and obtain the initial sea-surface elevation as the tsunami source. For example, one method divides the ocean of possible tsunami source area into small grids, imposes a unit water height of uniform or Gaussian shape at each grid, simulates the resulting tsunami waves and obtains the Green's functions at tsunami stations. By using the tsunami data recorded at these stations, a linear inversion is conducted to derive the water height at each grid, leading to the initial sea-surface elevation in the source region (e.g., Baba et al., 2005; Saito et al., 2010, 2011; Mulia and Asano, 2016). The advantage of this method is that it does not require prior information about the fault geometry and other earthquake source parameters. But at the same time, because of lacking constraints from fault and earthquake parameters, the degree of freedom is relatively large in the inversion. Thus, the inversion usually needs large smoothing and damping to obtain reasonable results. Another method of tsunami inversion is the time reversal method. This method reverses tsunami recordings in time, and applies them at tsunami stations in a numerical simulation. In the numerical simulation, tsunami waves propagate from stations to source. Tsunami waves from various stations interfere with each other and superimpose in the source region, and recover the tsunami source. The time reversal method was initially developed in acoustic research (Fink, 1992) and then had some applications in seismology (e.g., Tromp et al., 2005; Larmat et al., 2006). It was first introduced to tsunami research by Hossen et al. (2015b). Compared with seismic waves, the numerical simulation of tsunami waves is more accurate, so the method is theoretically more suitable for tsunami research. However, in reality, tsunami stations are usually sparse and the azimuthal coverage is poor, so it is often necessary to carefully select some tsunami stations for an acceptable reversal result (An and Meng, 2017; Hossen et al., 2018). Recently there are some studies that attempt to combine the time reversal method with inversion algorithm to improve the results (Hossen et al., 2015a; Zhou et al., 2019).

5. Tsunami warning

Tsunami warning consists of qualitative and quantitative levels, i.e., whether a tsunami is triggered by an earthquake, and the accurate prediction of tsunami arrival time and wave height (Table 1). After an earthquake, the hypocenter, depth and focal mechanism of the earthquake are estimated. Based on these parameters, the possibility of a tsunami is evaluated. Due to the saturation of seismometers, earthquake magnitude is not always well determined in a short time after an earthquake. For example, the magnitude of the 2011 Tohoku earthquake was largely underestimated in the initial analysis, which in turn led to underestimation of the tsunami (Hoshiba and Ozaki, 2014). Currently there are studies that attempt to constrain the earthquake magnitudes by utilizing other types of data, such as on-land geodetic data (Melgar et al., 2015) and ocean-bottom pressure data (An et al., 2017a; Kubota et al., 2017). Besides, the earthquake parameters that are obtained from fast estimation, such as earthquake magnitude, location and depth, are not directly related to the generation of tsunami waves, leading to frequent false warnings. As mentioned earlier, tsunami generation is directly related to seafloor deformation. Seafloor deformation produces sound waves in compressible seawater. Thus, it could be an effective solution to avoid false alarms by observing and judging if sound waves are generated by seafloor deformation after an earthquake. At present the theory and observation of water sound waves during earthquakes are still in development.

The tsunami scenario database is a widely adopted method for tsunami warning. The basic procedure is to construct a series of earthquake source models in areas with potential tsunami risks, with various earthquake magnitude, location and focal depth, simulate the tsunami waves and store the numerical results. After an earthquake occurs, according to the epicenter, focal depth and magnitude of the earthquake, the scenario with the most similar parameters is chosen to issue tsunami warnings. This method is adopted by the tsunami warning systems in many countries, such as in Japan (Kamigaichi, 2009), Australia (Greenslade and Titov, 2008; Greenslade et al., 2011) and Indonesia (Rudloff et al., 2009; Setiyono et al., 2017). To build a tsunami scenario database, it is required to construct rectangular uniform slip models based on earthquake magnitudes, and scaling relations are used to calculate the rupture length, width and area from earthquake magnitudes. In reality, earthquakes have non-uniform slip distributions, so it is generally believed that the assumption of uniform slip causes large prediction errors of tsunami waves. However, some studies constructed uniform slip models according to the rupture areas inferred from seismic back-projection analysis, and showed that these models led to acceptable tsunami predictions (An and Meng, 2016; Xie and Meng, 2020). An et al. (2018a) studied the 2011 Tohoku, 2014 Iquique and 2015 Illapel tsunamis and demonstrated that, if properly constructed, uniform slip models can accurately predict the tsunami waves, and the prediction accuracy is close to that of finite-fault models with heterogeneous slip. Thus, it is likely that tsunami prediction errors originate not from the assumption of uniform slip, but from inappropriate scaling relations used to construct the uniform slip models. Different tsunami warning systems use different scaling relations. The Japanese tsunami warning system operated by Japan Meteorological Agency (JMA) uses $\log L=0.5M_W-1.8$ and $L=2W$ (L, rupture length; W, rupture width; M_W, earthquake magnitude)(Kamigaichi, 2009). The T1 tsunami warning system in Australia assumes a length/width ratio between 2 to 10 for different earthquake magnitudes (Greenslade and Titov, 2008). The Indonesian tsunami warning system uses $M_W=4/3\log S+3.03$ and $L=2W$ (S, rupture area and $S=LW$) (Setiyono et al., 2017). These scaling relations, along with other commonly used scaling relations, such as those given by Wells and Coppersmith

Table 1 Tsunami warning strategies according to source distance and available observations[a)]

Distance	Observations	Task	Warning strategy	Problems	Possible solution
Very near field	Strong motion; geodetic	Whether a tsunami is triggered	Estimate earthquake hypocenter, magnitude and focal mechanism; determine if a tsunami occurs	Frequent false alarms	More near-source observations for direct evidence of a tsunami, e.g., ocean-bottom pressure
Near field & far field (without tsunamis)	Strong motion; geodetic; body waves; surface waves	Prediction of tsunami arrival time and wave height	(1) Use uniform slip models for prediction (e.g., tsunami scenarios) (2) Obtain finite-fault models by inversion	(1) Proper construction of uniform slip models (2) Finite-fault models based on seismic and geodetic data produce large errors to predict tsunami waves	Estimate the overall characteristics of earthquakes instead of detailed finite-fault models; use simplified source models for prediction of tsunami
Far field (with tsunamis)	Strong motion; geodetic; body waves; surface waves; tsunamis	Prediction of tsunami arrival time and wave height	Obtain finite-fault models by inversion of tsunami data and other data	Tsunami buoys are usually far from source. Near-field areas are not protected	More tsunami buoys in potential source areas

a) The principle criterion is whether tsunami data are available. Without tsunami data, one has to rely on seismic and geodetic data to estimate the earthquake rupture parameters, and then predict the tsunami waves. It is necessary to reduce the uncertainty of the estimation of source parameters in order to reduce tsunami prediction errors. If tsunami data are available, an inversion of tsunami data or a joint inversion of tsunami and other data can produce accurate tsunami predictions.

(1994), Strasser et al. (2010), Blaser et al. (2010) and Murotani et al. (2013), are mostly derived by analyzing the statistics of global earthquakes. Thus, they do not necessarily apply to large thrust earthquakes in subduction zones that excite tsunamis. An et al. (2018a) proposed a scaling relation with the main feature of a compacted rupture area, and claimed that it is suitable for tsunami predictions. The compacted rupture area is much smaller than the actual rupture area, and it is similar to the "asperity size" used by Murotani et al. (2013). Li et al. (2020) verified that this scaling relation leads to better tsunami predictions than other scaling relations for the 2011 Tohoku, 2014 Iquique and 2015 Illapel tsunamis.

In areas with tsunami buoys, tsunami warnings become accurate and reliable. The fundamental idea is to obtain earthquake finite-fault models by inversion of tsunami data, and then predict the tsunami waves. For instance, in the retrospective studies of several large tsunamis, the SIFT system developed by the Pacific Tsunami Warning Center (PTWC) has been demonstrated to be able to accurately reproduce the tsunami waves (Wei et al., 2008; Tang et al., 2016). At present, the number of tsunami buoys is still limited and more buoys are being deployed for warning purposes. Current strategies of tsunami buoy network design consist of various factors, such as bathymetry, ocean-bottom currents and political borders. And another important consideration is the distance from the buoy to trench, which should be as small as possible for early measurements and warning. Such a network design is helpful for fast warning purposes, but it does not necessarily lead to good constraints on earthquake source models by the tsunami measurements. Mulia et al. (2017a) suggested that tsunami buoys should be placed in the direction of tsunami energy radiation in order for best inversion results. An et al. (2018b) analyzed the 2011 Tohoku tsunami data and concluded that 2–4 tsunami buoys are sufficient to accurately constrain the earthquake source. They also gave the optimal locations to deploy tsunami buoys and the methodology to derive the optimal locations. Later there are more studies about the design of tsunami buoy network that considers prediction accuracy, warning delay and other factors (Meza et al., 2020; Mulia et al., 2019).

6. Probabilistic tsunami hazard assessment

Apart from tsunami warning, tsunami hazard assessment is also an important way of disaster mitigation. Traditional tsunami hazard assessment adopts deterministic methods. For a subduction zone with tsunami potential, the tsunami waves generated by the largest possible earthquake are numerically simulated, which is called "the worst scenario". Such assessment provides basis for coastal engineering design. If the evaluation of the probability of a tsunami exceeding a certain height in a certain region is needed, one has to conduct the Probabilistic Tsunami Hazard Assessment (PTHA, Geist and Parsons, 2006). PTHA generally calculates the probability of tsunamis due to the probability of earthquake occurrence. In a certain region, the number of earthquakes and earthquake magnitudes satisfy statistical relations, and hence a probability model can be developed to describe the future earthquakes in this region. Thereby, the probability of tsunamis can be obtained through numerical simulations (González et al., 2009; Sørensen et al., 2012). Later, scientists realize that for an earthquake of fixed magnitude, different focal depths and slip distributions also lead to different tsunami heights. Thus, in addition to the probability of earthquake occurrence, it is also necessary to consider the probability of earthquake focal depth and slip distribution when calculating the probability of tsunami height. Some studies adopt totally random slip distributions (Mueller et al., 2015), and later works generate slip distributions based on statistics of historic earthquakes (Goda et al., 2015; Li et al., 2016; Sepúlveda et al., 2017). One major problem with the PTHA method is that there are not sufficient earthquake records in a region to develop an accurate model of earthquake probability. Particularly, the maximum magnitude is not well determined, which affects the range of earthquake magnitude in the earthquake probability model. For instance, before the 2011 Tohoku earthquake, it was widely believed that the largest possible earthquake in the region was only 7.5 to 8.6 (Kagan and Jackson, 2013). Besides, further analysis is necessary to justify whether the slip distributions generated in PTHA analysis reflect the realistic probability of slip for future earthquakes. Grezio et al. (2017) provided a detailed review on the history, research progress, limitations and future prospects of PTHA. Generally speaking, current PTHA analysis adopts widely-used earthquake probability models. The G-R law that connects earthquake number and magnitude is obtained based on the earthquake catalog in the studied area, and hence different areas have different earthquake probability models. However, additional information of local geological structures is not fully utilized. For example, most PTHA studies assume that earthquakes are uniformly distributed in the studied area. Future PTHA may improve the spatial distributions of earthquakes by taking into account research results of plate coupling, numerical simulations of earthquake circles, etc.

7. Conclusions and future prospects

This paper reviews the research of tsunamis generated by subduction earthquakes in the aspects of generation, propagation, inversion and warning. The main conclusions are summarized as follows.

(1) Since the 2004 Sumatra tsunami, there have been more and more tsunami measurements. A lot of research has been done and the research methodologies have been well developed. With the deployment of ocean-bottom pressure sensors, it becomes possible to study the response of compressible seawater during earthquakes. Ocean-bottom pressure data contain information about the physical process of transmission of seismic waves at solid-fluid interface, generation of water sound waves and generation of tsunamis. It is possibly useful for the development of reliable tsunami warning strategies. This is expected to be a hot research topic in the future.

(2) By far tsunami buoys are still the most reliable ways of tsunami warning. If tsunami measurements are not available, finite-fault models obtained by inversion of seismic and geodetic data may lead to large tsunami prediction errors. One possible solution is to estimate the overall characteristics of earthquakes, such as magnitude, depth, rupture extent, and then use simplified uniform models to predict tsunami waves.

(3) Probabilistic methods are developed for tsunami hazard assessment in addition to traditional deterministic methods. Various uncertainties in tsunami simulations, especially uncertainties of earthquake source parameters, are converted to uncertainties of tsunami height through PTHA analysis. Correct evaluation of earthquake source uncertainties is of essential importance to PTHA analysis. Future improvement can be made by implementing more research results in seismology, such as plate coupling, numerical simulations of earthquake circles, etc.

Acknowledgements *The author thanks all the researchers who contribute to the research of tsunamis, tsunami warning, tsunami hazard assessment and data sharing. Tsunami research benefits from the data service provided by many institutes such as NOAA and IOC. This work was supported by the National Natural Science Foundation of China (Grant Nos. U1901602, 11632012).*

References

An C, Cai C, Zheng Y, Meng L, Liu P. 2017a. Theoretical solution and applications of ocean bottom pressure induced by seismic seafloor motion. Geophys Res Lett, 44: 10272–210281

An C, Liu P L F. 2014. Characteristics of leading tsunami waves generated in three recent tsunami events. J Earthq Tsunami, 08: 1440001

An C, Liu P L F. 2016. Analytical solutions for estimating tsunami propagation speeds. Coast Eng, 117: 44–56

An C, Liu P L F, Meng L. 2018b. A sensitivity analysis of tsunami inversions on the number of stations. Geophys J Int, 214: 1313–1323

An C, Liu H, Ren Z, Yuan Y. 2018a. Prediction of tsunami waves by uniform slip models. J Geophys Res-Oceans, 123: 8366–8382

An C, Meng L. 2016. Application of array backprojection to tsunami prediction and early warning. Geophys Res Lett, 43: 3677–3685

An C, Meng L. 2017. Time reversal imaging of the 2015 Illapel tsunami source. Geophys Res Lett, 44: 1732–1739

An C, Sepúlveda I, Liu P L F. 2014. Tsunami source and its validation of the 2014 Iquique, Chile, earthquake. Geophys Res Lett, 41: 3988–3994

An C, Yue H, Sun J, Meng L, Báez J C. 2017b. The 2015 M_W8.3 Illapel, Chile, earthquake: Direction-reversed along-dip rupture with localized water reverberation. Bull Seismol Soc Am, 107: 2416–2426

Baba T, Allgeyer S, Hossen J, Cummins P R, Tsushima H, Imai K, Yamashita K, Kato T. 2017. Accurate numerical simulation of the far-field tsunami caused by the 2011 Tohoku earthquake, including the effects of Boussinesq dispersion, seawater density stratification, elastic loading, and gravitational potential change. Ocean Model, 111: 46–54

Baba T, Cummins P R. 2005. Contiguous rupture areas of two Nankai Trough earthquakes revealed by high-resolution tsunami waveform inversion. Geophys Res Lett, 32: L08305

Baba T, Cummins R, Hori T. 2005. Compound fault rupture during the 2004 off the Kii Peninsula earthquake (*M*7.4) inferred from highly resolved coseismic sea-surface deformation. Earth Planet Sp, 57: 167–172

Baba T, Tanioka Y, Cummins P R, Uhira K. 2002. The slip distribution of the 1946 Nankai earthquake estimated from tsunami inversion using a new plate model. Phys Earth Planet Inter, 132: 59–73

Blaser L, Kruger F, Ohrnberger M, Scherbaum F. 2010. Scaling relations of earthquake source parameter estimates with special focus on subduction environment. Bull Seismol Soc Am, 100: 2914–2926

Fink M. 1992. Time reversal of ultrasonic fields. I. Basic principles. IEEE Trans Ultrason Ferroelect Freq Contr, 39: 555–566

Fujii Y, Satake K. 2007. Tsunami source of the 2004 Sumatra-Andaman earthquake inferred from tide gauge and satellite data. Bull Seismol Soc Am, 97: S192–S207

Fujii Y, Satake K. 2013. Slip distribution and seismic moment of the 2010 and 1960 Chilean earthquakes inferred from tsunami waveforms and coastal geodetic data. Pure Appl Geophys, 170: 1493–1509

Fujii Y, Satake K, Sakai S, Shinohara M, Kanazawa T. 2011. Tsunami source of the 2011 off the Pacific coast of Tohoku Earthquake. Earth Planet Sp, 63: 815–820

Geist E L, Parsons T. 2006. Probabilistic analysis of tsunami hazards. Nat Hazards, 37: 277–314

Goda K, Yasuda T, Mori N, Mai P M. 2015. Variability of tsunami inundation footprints considering stochastic scenarios based on a single rupture model: Application to the 2011 Tohoku earthquake. J Geophys Res-Oceans, 120: 4552–4575

González F I, Geist E L, Jaffe B, Kânoğlu U, Mofjeld H, Synolakis C E, Titov V V, Arcas D, Bellomo D, Carlton D, Horning T, Johnson J, Newman J, Parsons T, Peters R, Peterson C, Priest G, Venturato A, Weber J, Wong F, Yalciner A. 2009. Probabilistic tsunami hazard assessment at seaside, Oregon, for near- and far-field seismic sources. J Geophys Res, 114: C11023

Greenslade D J M, Allen S C R, Simanjuntak M A. 2011. An evaluation of tsunami forecasts from the T2 scenario database. Pure Appl Geophys, 168: 1137–1151

Greenslade D J M, Titov V V. 2008. A comparison study of two numerical tsunami forecasting systems. Pure Appl Geophys, 165: 1991–2001

Grezio A, Babeyko A, Baptista M A, Behrens J, Costa A, Davies G, Geist E L, Glimsdal S, González F I, Griffin J, Harbitz C B, LeVeque R J, Lorito S, Løvholt F, Omira R, Mueller C, Paris R, Parsons T, Polet J, Power W, Selva J, Sørensen M B, Thio H K. 2017. Probabilistic tsunami hazard analysis: Multiple sources and global applications. Rev Geophys, 55: 1158–1198

Grilli S T, Ioualalen M, Asavanant J, Shi F, Kirby J T, Watts P. 2007. Source constraints and model simulation of the December 26, 2004, Indian Ocean Tsunami. J Waterway Port Coast Ocean Eng, 133: 414–428

Grilli S T, Tappin D R, Carey S, Watt S F L, Ward S N, Grilli A R, Engwell S L, Zhang C, Kirby J T, Schambach L, Muin M. 2019. Modelling of the tsunami from the December 22, 2018 lateral collapse of Anak Krakatau volcano in the Sunda Straits, Indonesia. Sci Rep, 9: 1–3

Gusman A R, Tanioka Y, Sakai S, Tsushima H. 2012. Source model of the great 2011 Tohoku earthquake estimated from tsunami waveforms and crustal deformation data. Earth Planet Sci Lett, 341-344: 234–242

Heidarzadeh M, Murotani S, Satake K, Ishibe T, Gusman A R. 2016. Source model of the 16 September 2015 Illapel, Chile, M_W8.4 earthquake based on teleseismic and tsunami data. Geophys Res Lett, 43:

643–650
Ho T C, Satake K, Watada S. 2017. Improved phase corrections for transoceanic tsunami data in spatial and temporal source estimation: Application to the 2011 Tohoku earthquake. J Geophys Res-Solid Earth, 122: 10155
Ho T C, Satake K, Watada S, Fujii Y. 2019. Source estimate for the 1960 Chile earthquake from joint inversion of geodetic and transoceanic tsunami data. J Geophys Res-Solid Earth, 124: 2812–2828
Hoshiba M, Ozaki T. 2014. Earthquake early warning and tsunami warning of the Japan Meteorological Agency and their performance in the 2011 off the Pacific coast of Tohoku earthquake (M_W9.0). In: Wenzel F, Zschau J, eds. Early Warning for Geological Disasters. Berlin: Springer. 1–28
Hossen M J, Cummins P R, Dettmer J, Baba T. 2015a. Time reverse imaging for far-field tsunami forecasting: 2011 Tohoku earthquake case study. Geophys Res Lett, 42: 9906–9915
Hossen M J, Cummins P R, Roberts S G, Allgeyer S. 2015b. Time reversal imaging of the tsunami source. Pure Appl Geophys, 172: 969–984
Hossen M J, Gusman A, Satake K, Cummins P R. 2018. An adjoint sensitivity method applied to time reverse imaging of tsunami source for the 2009 Samoa earthquake. Geophys Res Lett, 45: 627–636
Hsu Y J, Yu S B, Loveless J P, Bacolcol T, Solidum R, Luis Jr A, Pelicano A, Woessner J. 2016. Interseismic deformation and moment deficit along the Manila subduction zone and the Philippine Fault system. J Geophys Res-Solid Earth, 121: 7639–7665
Hsu Y J, Yu S B, Song T R A, Bacolcol T. 2012. Plate coupling along the Manila subduction zone between Taiwan and northern Luzon. J Asian Earth Sci, 51: 98–108
Hu C, Wu Y, An C, Liu H. 2020. A numerical study of tsunami generation by horizontal displacement of sloping seafloor. J Earthq Tsunami, 14: 2050018
Imamura F. 1996. Simulation of wave-packet propagation along sloping beach by TUNAMI-code. In: Yeh H, Liu P L, Synolakis C, eds. Long-wave Runup Models. Friday Harbor: World Scientific. 231–241
Ishii M, Shearer P M, Houston H, Vidale J E. 2005. Extent, duration and speed of the 2004 Sumatra-Andaman earthquake imaged by the Hi-Net array. Nature, 435: 933–936
Kagan Y Y, Jackson D D. 2013. Tohoku earthquake: A surprise? Bull Seismol Soc Am, 103: 1181–1194
Kajiura K. 1963. The leading wave of a tsunami. Bulletin of the Earthquake Research Institute, University of Tokyo, 41: 535–571
Kajiura K. 1970. Tsunami source, energy and the directivity of wave radiation. Bulletin of the Earthquake Research Institute, University of Tokyo, 48: 835–869
Kajiura K. 1981. Tsunami energy in relation to parameters of the earthquake fault model. Bulletin of the Earthquake Research Institute, University of Tokyo, 56: 415–440
Kamigaichi O. 2009. Tsunami forecasting and warning. In: Meyers R A, ed. Extreme Environmental Events. New York: Springer. 9592–9618
Kubota T, Saito T, Suzuki W, Hino R. 2017. Estimation of seismic centroid moment tensor using ocean bottom pressure gauges as seismometers. Geophys Res Lett, 44: 10,907
Larmat C, Montagner J P, Fink M, Capdeville Y, Tourin A, Clévédé E. 2006. Time-reversal imaging of seismic sources and application to the great Sumatra earthquake. Geophys Res Lett, 33: L19312
Lay T, Kanamori H, Ammon C J, Nettles M, Ward S N, Aster R C, Beck S L, Bilek S L, Brudzinski M R, Butler R, DeShon H R, Ekström G, Satake K, Sipkin S. 2005. The great Sumatra-Andaman earthquake of 26 December 2004. Science, 308: 1127–1133
Lay T, Yue H, Brodsky E E, An C. 2014. The 1 April 2014 Iquique, Chile, M_W8.1 earthquake rupture sequence. Geophys Res Lett, 41: 3818–3825
LeVeque R J, George D L, Berger M J. 2011. Tsunami modelling with adaptively refined finite volume methods. Acta Numerica, 20: 211–289
Li L, Switzer A D, Chan C H, Wang Y, Weiss R, Qiu Q. 2016. How heterogeneous coseismic slip affects regional probabilistic tsunami hazard assessment: A case study in the South China Sea. J Geophys Res-Solid Earth, 121: 6250–6272
Li Z, An C, Liu H. 2020. Evaluation of different earthquake scaling relations on the generation of tsunamis and hazard assessment. Ocean Eng, 195: 106716
Liu P L F, Lynett P, Fernando H, Jaffe B E, Fritz H, Higman B, Morton R, Goff J, Synolakis C. 2005. Observations by the international tsunami survey team in Sri Lanka. Science, 308: 1595
Liu P L F, Wang X, Salisbury A J. 2009. Tsunami hazard and early warning system in South China Sea. J Asian Earth Sci, 36: 2–12
Liu P L F, Woo S B, Cho Y S. 1998. Computer programs for tsunami propagation and inundation. Technical Report. Cornell University
Liu Y, Santos A, Wang S M, Shi Y, Liu H, Yuen D A. 2007. Tsunami hazards along Chinese coast from potential earthquakes in South China Sea. Phys Earth Planet Inter, 163: 233–244
Lotto G C, Nava G, Dunham E M. 2017. Should tsunami simulations include a nonzero initial horizontal velocity? Earth Planets Space, 69: 117
Lynett P, Liu P, Sitanggang K, Kim D. 2002. Modeling wave generation, evolution, and interaction with depth-integrated, dispersive wave equations COULWAVE Code Manual
Megawati K, Shaw F, Sieh K, Huang Z, Wu T R, Lin Y, Tan S K, Pan T C. 2009. Tsunami hazard from the subduction megathrust of the South China Sea: Part I. Source characterization and the resulting tsunami. J Asian Earth Sci, 36: 13–20
Mei C C. 1989. The Applied Dynamics of Ocean Surface Waves. London: World Scientific. 611
Mei C C, Kadri U. 2018. Sound signals of tsunamis from a slender fault. J Fluid Mech, 836: 352–373
Melgar D, Crowell B W, Geng J, Allen R M, Bock Y, Riquelme S, Hill E M, Protti M, Ganas A. 2015. Earthquake magnitude calculation without saturation from the scaling of peak ground displacement. Geophys Res Lett, 42: 5197–5205
Meza J, Catalán P A, Tsushima H. 2020. A multiple-parameter methodology for placement of tsunami sensor networks. Pure Appl Geophys, 177: 1451–1470
Monecke K, Finger W, Klarer D, Kongko W, McAdoo B G, Moore A L, Sudrajat S U. 2008. A 1,000-year sediment record of tsunami recurrence in northern Sumatra. Nature, 455: 1232–1234
Mueller C, Power W, Fraser S, Wang X. 2015. Effects of rupture complexity on local tsunami inundation: Implications for probabilistic tsunami hazard assessment by example. J Geophys Res-Solid Earth, 120: 488–502
Mulia I E, Asano T. 2016. Initial tsunami source estimation by inversion with an intelligent selection of model parameters and time delays. J Geophys Res-Oceans, 121: 441–456
Mulia I E, Gusman A R, Satake K. 2017a. Optimal design for placements of tsunami observing systems to accurately characterize the inducing earthquake. Geophys Res Lett, 44: 12,106
Mulia I E, Gusman A R, Williamson A L, Satake K. 2019. An optimized array configuration of tsunami observation network off Southern Java, Indonesia. J Geophys Res-Solid Earth, 124: 9622–9637
Mulia I E, Inazu D, Waseda T, Gusman A R. 2017b. Preparing for the future Nankai Trough tsunami: A data assimilation and inversion analysis from various observational systems. J Geophys Res-Oceans, 122: 7924–7937
Murotani S, Satake K, Fujii Y. 2013. Scaling relations of seismic moment, rupture area, average slip, and asperity size for M~9 subduction-zone earthquakes. Geophys Res Lett, 40: 5070–5074
Nakamura M. 2009. Fault model of the 1771 Yaeyama earthquake along the Ryukyu Trench estimated from the devastating tsunami. Geophys Res Lett, 36: L19307
Namegaya Y, Satake K. 2014. Reexamination of the AD 869 Jogan earthquake size from tsunami deposit distribution, simulated flow depth, and velocity. Geophys Res Lett, 41: 2297–2303
Nanayama F, Satake K, Furukawa R, Shimokawa K, Atwater B F, Shigeno K, Yamaki S. 2003. Unusually large earthquakes inferred from tsunami deposits along the Kuril trench. Nature, 424: 660–663
Nosov M A. 1999. Tsunami generation in compressible ocean. Phys Chem

Earth Part B, 24: 437–441
Nosov M A, Kolesov S V. 2007. Elastic oscillations of water column in the 2003 Tokachi-oki tsunami source: *In-situ* measurements and 3-D numerical modelling. Nat Hazards Earth Syst Sci, 7: 243–249
Okada Y. 1985. Surface deformation due to shear and tensile faults in a half-space. Bull Seismol Soc Am, 75: 1135–1154
Ren Z Y, Liu H, Wang B L, Zhao X. 2014. An investigation on multi-buoy inversion method for tsunami warning system in South China Sea. J Earthq Tsunami, 08: 1440004
Ren Z, Liu H, Zhao X, Wang B, An C. 2019. Effect of kinematic fault rupture process on tsunami propagation. Ocean Eng, 181: 43–58
Rudloff A, Lauterjung J, Münch U, Tinti S. 2009. Preface "The GITEWS Project (German-Indonesian Tsunami Early Warning System)". Nat Hazards Earth Syst Sci, 9: 1381–1382
Saito T. 2013. Dynamic tsunami generation due to sea-bottom deformation: Analytical representation based on linear potential theory. Earth Planet Sp, 65: 1411–1423
Saito T. 2017. Tsunami generation: Validity and limitations of conventional theories. Geophys J Int, 210: 1888–1900
Saito T, Inazu D, Miyoshi T, Hino R. 2014. Dispersion and nonlinear effects in the 2011 Tohoku-Oki earthquake tsunami. J Geophys Res-Oceans, 119: 5160–5180
Saito T, Ito Y, Inazu D, Hino R. 2011. Tsunami source of the 2011 Tohoku-Oki earthquake, Japan: Inversion analysis based on dispersive tsunami simulations. Geophys Res Lett, 38: L00G19
Saito T, Satake K, Furumura T. 2010. Tsunami waveform inversion including dispersive waves: The 2004 earthquake off Kii Peninsula, Japan. J Geophys Res, 115: B06303
Saito T, Tsushima H. 2016. Synthesizing ocean bottom pressure records including seismic wave and tsunami contributions: Toward realistic tests of monitoring systems. J Geophys Res-Solid Earth, 121: 8175–8195
Satake K. 1987. Inversion of tsunami waveforms for the estimation of a fault heterogeneity: Method and numerical experiments. J Phys Earth, 35: 241–254
Satake K. 1993. Depth distribution of coseismic slip along the Nankai Trough, Japan, from joint inversion of geodetic and tsunami data. J Geophys Res, 98: 4553–4565
Satake K, Fujii Y, Harada T, Namegaya Y. 2013. Time and space distribution of coseismic slip of the 2011 Tohoku earthquake as inferred from tsunami waveform data. Bull Seismol Soc Am, 103: 1473–1492
Satake K, Heidarzadeh M, Quiroz M, Cienfuegos R. 2020. History and features of trans-oceanic tsunamis and implications for paleo-tsunami studies. Earth-Sci Rev, 202: 103112
Satake K, Shimazaki K, Tsuji Y, Ueda K. 1996. Time and size of a giant earthquake in Cascadia inferred from Japanese tsunami records of January 1700. Nature, 379: 246–249
Sepúlveda I, Liu P L F, Grigoriu M, Pritchard M. 2017. Tsunami hazard assessments with consideration of uncertain earthquake slip distribution and location. J Geophys Res-Solid Earth, 122: 7252–7271
Setiyono U, Gusman A R, Satake K, Fujii Y. 2017. Pre-computed tsunami inundation database and forecast simulation in Pelabuhan Ratu, Indonesia. Pure Appl Geophys, 174: 3219–3235
Shi F, Kirby J T, Harris J C, Geiman J D, Grilli S T. 2012. A high-order adaptive time-stepping TVD solver for Boussinesq modeling of breaking waves and coastal inundation. Ocean Model, 43-44: 36–51
Simkin T, Fiske R S. 1983. Krakatau, 1883: The Volcanic Eruption and its Effects. Washington DC: Smithsonian Institution Press
Simons M, Minson S E, Sladen A, Ortega F, Jiang J, Owen S E, Meng L, Ampuero J P, Wei S, Chu R, Helmberger D V, Kanamori H, Hetland E, Moore A W, Webb F H. 2011. The 2011 magnitude 9.0 Tohoku-Oki earthquake: Mosaicking the megathrust from seconds to centuries. Science, 332: 1421–1425
Song Y T, Fu L L, Zlotnicki V, Ji C, Hjorleifsdottir V, Shum C K, Yi Y. 2008. The role of horizontal impulses of the faulting continental slope in generating the 26 December 2004 tsunami. Ocean Model, 20: 362–379
Song Y T, Mohtat A, Yim S C. 2017. New insights on tsunami genesis and energy source. J Geophys Res-Oceans, 122: 4238–4256
Sørensen M B, Spada M, Babeyko A, Wiemer S, Grünthal G. 2012. Probabilistic tsunami hazard in the Mediterranean Sea. J Geophys Res, 117: B01305
Strasser F O, Arango M C, Bommer J J. 2010. Scaling of the source dimensions of interface and intraslab subduction-zone earthquakes with moment magnitude. Seismol Res Lett, 81: 941–950
Sun L, Zhou X, Huang W, Liu X, Yan H, Xie Z, Wu Z, Zhao S, Da Shao S, Yang W. 2013. Preliminary evidence for a 1000-year-old tsunami in the South China Sea. Sci Rep, 3: 1655
Tang L, Titov V V, Moore C, Wei Y. 2016. Real-time assessment of the 16 September 2015 Chile tsunami and implications for near-field forecast. Pure Appl Geophys, 173: 369–387
Tanioka Y, Satake K. 1996. Tsunami generation by horizontal displacement of ocean bottom. Geophys Res Lett, 23: 861–864
Tanioka Y, Satake K. 2001a. Coseismic slip distribution of the 1946 Nankai earthquake and aseismic slips caused by the earthquake. Earth Planet Sp, 53: 235–241
Tanioka Y, Satake K. 2001b. Detailed coseismic slip distribution of the 1944 Tonankai earthquake estimated from tsunami waveforms. Geophys Res Lett, 28: 1075–1078
Tanioka Y, Seno T. 2001. Sediment effect on tsunami generation of the 1896 Sanriku tsunami earthquake. Geophys Res Lett, 28: 3389–3392
Titov V V, Gonzalez F I. 1997. Implementation and testing of the method of splitting tsunami (MOST) model. NOAA Technical Memorandum ERL PMEL-112
Titov V, Rabinovich A B, Mofjeld H O, Thomson R E, González F I. 2005. The global reach of the 26 December 2004 Sumatra tsunami. Science, 309: 2045–2048
Titov V V, Synolakis C E. 1998. Numerical modeling of tidal wave runup. J Waterway Port Coast Ocean Eng, 124: 157–171
Tromp J, Tape C, Liu Q. 2005. Seismic tomography, adjoint methods, time reversal and banana-doughnut kernels. Geophys J Int, 160: 195–216
Tsai V C, Ampuero J P, Kanamori H, Stevenson D J. 2013. Estimating the effect of Earth elasticity and variable water density on tsunami speeds. Geophys Res Lett, 40: 492–496
Wang X, Liu P L F. 2006. An analysis of 2004 Sumatra earthquake fault plane mechanisms and Indian Ocean tsunami. J Hydraul Res, 44: 147–154
Watada S. 2013. Tsunami speed variations in density-stratified compressible global oceans. Geophys Res Lett, 40: 4001–4006
Watada S, Kusumoto S, Satake K. 2014. Traveltime delay and initial phase reversal of distant tsunamis coupled with the self-gravitating elastic Earth. J Geophys Res-Solid Earth, 119: 4287–4310
Watanabe S, Bock Y, Melgar D, Tadokoro K. 2018. Tsunami scenarios based on interseismic models along the Nankai trough, Japan, from seafloor and onshore geodesy. J Geophys Res-Solid Earth, 123: 2448–2461
Wei Y, Bernard E N, Tang L, Weiss R, Titov V V, Moore C, Spillane M, Hopkins M, Kânoğlu U. 2008. Real-time experimental forecast of the Peruvian tsunami of August 2007 for U.S. coastlines. Geophys Res Lett, 35: L04609
Wells D L, Coppersmith K J. 1994. New empirical relationships among magnitude, rupture length, rupture width, rupture area, and surface displacement. Bull Seismol Soc Am, 84: 974–1002
Williams R, Rowley P, Garthwaite M C. 2019. Reconstructing the Anak Krakatau flank collapse that caused the December 2018 Indonesian tsunami. Geology, 47: 973–976
Wu W. 1982. Fluid Mechanics. Beijing: Peking University Press
Xie Y, Meng L. 2020. A multi-array back-projection approach for tsunami warning. Geophys Res Lett, 47: e85763
Yamaguchi D K, Atwater B F, Bunker D E, Benson B E, Reid M S. 1997. Tree-ring dating the 1700 Cascadia earthquake. Nature, 389: 922–923
Yang W, Zhou X, Xiang R, Wang Y, Sun L. 2017. Palaeotsunami in the East China Sea for the past two millennia: A perspective from the

sedimentary characteristics of mud deposit on the continental shelf. Quat Int, 452: 54–64

Yang W, Sun L, Yang Z, Gao S, Gao Y, Shao D, Mei Y, Zang J, Wang Y, Xie Z. 2019. Nan'ao, an archaeological site of Song dynasty destroyed by tsunami (in Chinese). Chin Sci Bull, 64: 107–120

Yue H, Lay T, Rivera L, An C, Vigny C, Tong X, Báez Soto J C. 2014. Localized fault slip to the trench in the 2010 Maule, Chile M_W=8.8 earthquake from joint inversion of high-rate GPS, teleseismic body waves, InSAR, campaign GPS, and tsunami observations. J Geophys Res-Solid Earth, 119: 7786–7804

Yue H, Zhang Y, Ge Z, Wang T, Zhao L. 2020. Resolving rupture processes of great earthquakes: Reviews and perspective from fast response to joint inversion. Sci China Earth Sci, 63: 492–511

Zhou T, Meng L, Xie Y, Han J. 2019. An adjoint-state full-waveform tsunami source inversion method and its application to the 2014 Chile-Iquique tsunami event. J Geophys Res-Solid Earth, 124: 6737–6750

(Responsible editor: Yong ZHENG)